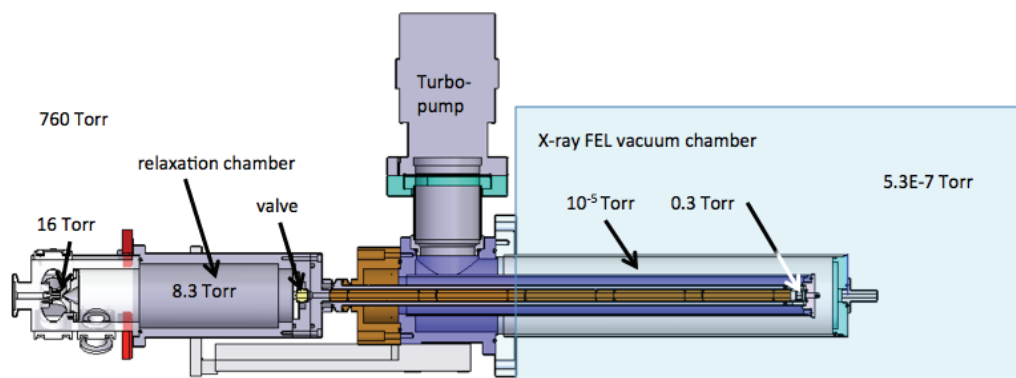
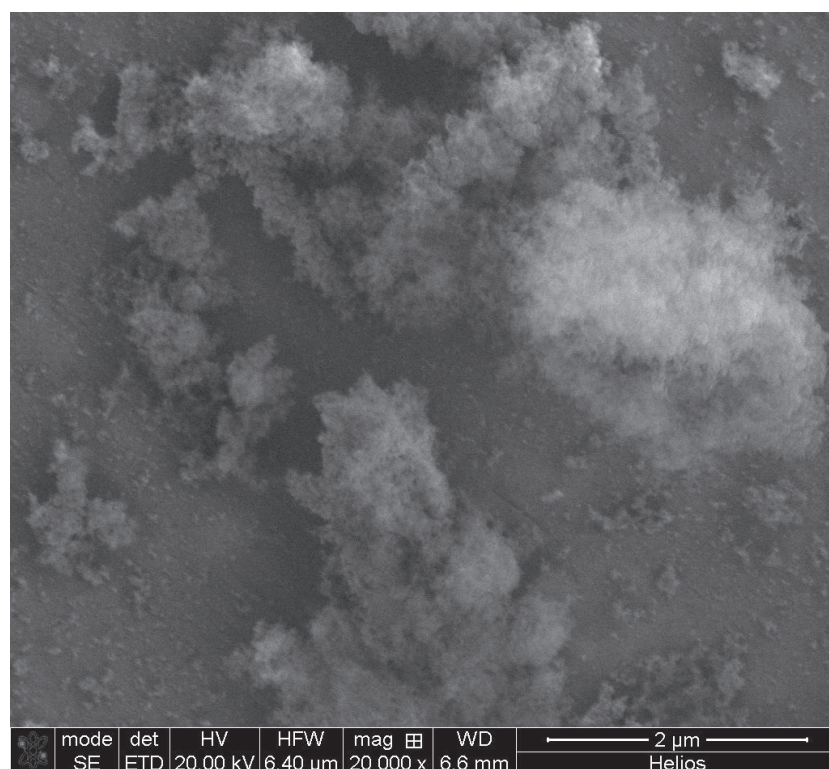


Supplementary Figures and Legends 1-4

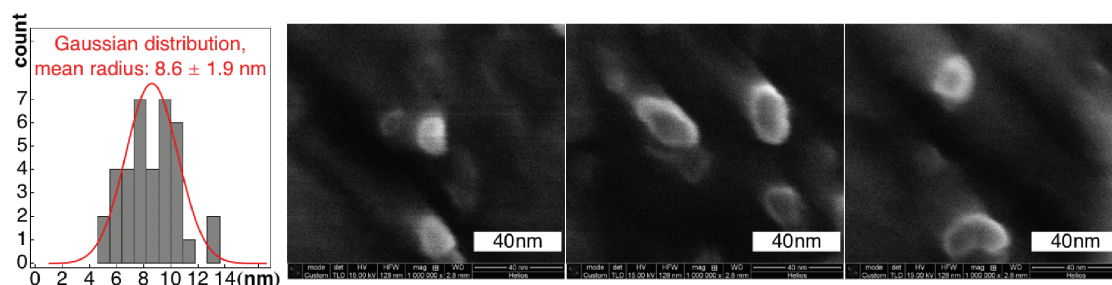


Supplementary Figure 1. A cross-section schematic of the aerodynamic lens stack. Aerosols were generated at the inlet (left) using a soot generator, a pneumatically-assisted sprayer, or a jet nebulizer containing a dry powder that is dispersed via agitation of the nebulizer and collisions with milling objects and then transferred to the lens stack aerosol inlet via a stream of 2 l/min compressed gas. Mixed aerosols such as soot+NaCl aggregates were obtained by directing two separate aerosol streams into a relaxation chamber located immediately before the aerosol inlet of the lens stack as shown in this Figure. The particle beam exits at the right into the vacuum chamber where it intersects with the FEL pulses.

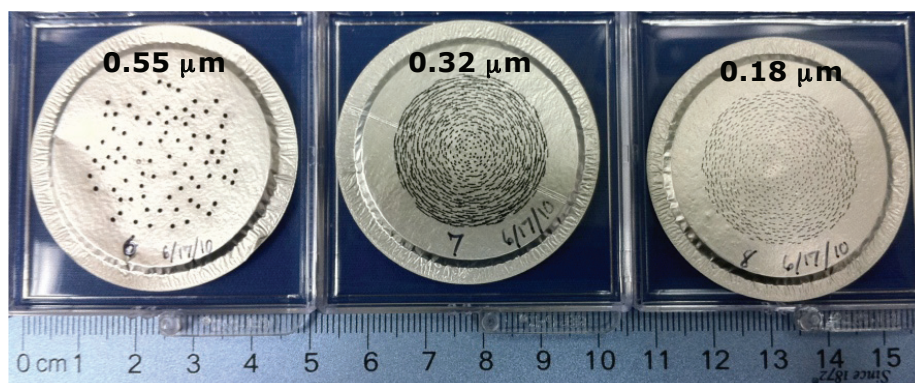


Supplementary Figure 2. A scanning electron micrograph of dense soot aggregates similar to those injected into the FEL beam. These soot aggregates were generated from a spark-generated source under the same conditions as those in our FEL experiment and

were captured on an aluminum foil after a MOUDI size selector. The scanning electron microscopy parameters are abbreviated in the Figure.



Supplementary Figure 3. Sizing primary particles in soot aggregates. Figure shows three of scanning electron micrographs used to estimate the minimum lengths of persistent spherical features in soot primary particles (scale bar in white). This was taken to be the radius of the semi-minor axis of misshapen primary particles r_{sp} such as those shown in this Figure. The distribution of monomer radii in larger soot aggregates was assumed to be equivalent to the distribution of r_{sp} (plot on the left).



Supplementary Figure 4. Soot particles captured by the MOUDI.

Supplementary Methods

Experimental setup

Aerosols were accelerated to the X-ray free-electron laser (FEL) interaction region by a differentially pumped re-entrant aerodynamic focusing inlet that was mounted on the CFEL-ASG Multi-Purpose (CAMP) instrument¹⁹ at the Atomic, Molecular and Optical Science beam line²⁰ of the Linac Coherent Light Source⁶ (LCLS) in Stanford, California. Particles exiting the inlet traveled 22 mm through vacuum to the interaction region with a velocity of 100–200 m/s and were randomly intercepted in the center of a time-of-flight mass spectrometer²⁴ by LCLS X-ray pulses sent at a rate of 60 Hz. Conically shaped spectrometer electrodes allow a free line of sight from the interaction region to the photon detector. Far-field diffraction patterns were recorded at low pressure (7×10^{-7} mbar) to minimize background scattering. The diffraction data in this paper were collected with single X-ray pulses comprising 1.0 nm wavelength radiation at fluences up to 2.1×10^{12} photons per pulse (13.5% beam line transmission with entrant photon pulse energy of 3.0 mJ), focused to about $10 \mu\text{m}^2$ giving a maximum of 2.1×10^{11} photons/ μm^2 in the center of this beam in the interaction region (peak power density of 2.8×10^{16} W/ cm^2), and compressed to a photon pulse length shorter than the 150 fs FWHM pulse duration of the electron bunches.

Forward-scattered diffraction patterns were recorded on a pair of pn-junction charge-coupled device¹⁹ (pnCCD) detectors at 60 Hz, matching the arrival rate of LCLS pulses. The active area for each detector half was $76.8 \times 38.4 \text{ mm}^2$, containing 1024×512 pixels each with $75 \times 75 \mu\text{m}^2$ dimensions. Of the recorded patterns, only those with substantially more integrated signal than a running average background were later examined as candidate hits. The detector pair was placed 721 mm downstream of the interaction point, giving a maximum full-period resolution of approximately 13 nm at the corners the compound detector (19 nm at the detector's edge) when imaging with 1.2 keV (1.0 nm) photons; the detector's quantum efficiency was estimated as 90%¹⁹. The direct beam exited through an opening between the two detector halves, and was absorbed in a beam dump behind the detectors.

Time of flight mass spectrometry (TOF-MS)

Fragment ion time-of-flight mass spectra were recorded with the CAMP velocity map imaging (VMI) spectrometer¹⁹ operated in a non-focusing time-of-flight mode. Extraction voltages of $\pm 1000 \text{ V}$ were applied to the conically shaped repeller and extractor electrodes (corresponding to an extraction field of roughly 570 V/cm), and -1000 V to all other electrodes and the drift tube. After a flight distance of 21 cm from the interaction point, the fragment ions were accelerated to 2000V for the detection on a microchannel plate (MCP) detector. The MCP signal trace comprising many hundreds to thousands of ion was then recorded for each FEL shot with an Acqiris digitizer.

Aerodynamic lens particle inlet

A re-entrant aerodynamic focusing inlet previously used for single-particle diffraction imaging at FLASH was used^{21,23,24}. The entire 3-stage differential pumping stage that houses the aerodynamic lens can be mechanically translated to enable steering of the particle beam towards the X-ray interaction region (Figure S1). A valve controlled the effective pumping speed in the first differential pumping stage, a pressure flow reducer²³. This enables optimization of the particle transmission with pressure. The pressure flow reducer consists of a nozzle/skimmer assembly described in more detail elsewhere^{23,32}. An inlet valve is positioned at the end of the relaxation chamber, enabling the CAMP¹⁹ chamber to be isolated from the relaxation chamber and nozzle/skimmer assembly.

The divergence angle of the particle beam exiting the aerodynamic focusing inlet was measured by visual inspection of 70 nm radius polystyrene spheres (6×10^9 particles/mL; PostNova Analytics, Germany) deposited onto a greased silicon wafer at two known positions. Note that this divergence angle may depend on samples. A disposable nebulizer (Salter Labs, Arvin, CA) was used to aerosolize 5 ml of sample with a stream of air (flow rate of 0–2.75 l/min) and a sample consumption rate of 35 μ l/min. The beam divergence was determined to be 0.57° which results in a particle beam spot diameter of approximately 440 μ m at the X-ray interaction region. Alignment of the aerodynamic lens stack relative to the interaction region was accomplished with an X,Y-translation stage that was controlled via electronic motors (MDrive23Plus, Schneider Electric, Marlborough, CT) in the FEL beam's propagation direction and vertically across it. A small removable 1 mm fiducial is attached to the end of the lens stack and aligned vertically to the AMO beamline HeNe alignment laser prior to the X-ray experiment.

Aerosol Generation and Characteristics

Soot-like aggregate particles were generated from a Palas GFG1000 spark source generator (Karlsruhe, Germany) containing two graphite electrodes separated by a fixed 2 mm gap. Argon flowing at 4 l/min was used to sustain the discharge and transport the particles to the exit of the generator yielding soot mass transport ranging from 2.1 to 6.1 mg/hour. Figure S2 shows dense soot aggregates produced by this mechanism. Our low Argon gas flow rate is responsible for the remarkably large monomer sizes in our soot particles³³ (Figure S3). Soot aerosols were either directly transported into the lens stack for X-ray diffraction imaging, size-separated using an inertial impactor, or mixed with an aerosolized NaCl solution in a mixing chamber followed by diffraction imaging.

Spark-generated soot particles were found to comprise primary particles that were smooth monomers of amorphous carbon³. Since we were interested in the scattering intensities of the positions of the monomers within the mass fractal, we needed to verify that the monomer shape minimally affects our diffraction intensities. We estimated the distribution of soot monomer radii by measuring the minimum sizes of their spherical features in scanning electron micrographs in Figure S3 and found their radii to be (8.6 ± 1.9) nm. Hence, to minimize scattering effects from the monomer shapes, we avoided scattering vectors q that were larger than $(2\pi/18)$ nm⁻¹ in our fractal morphology measurements.

Cross-flow mixing of particles such as soot and NaCl was carried out by directing aerosols of two distinct samples into a KF25 tee and sampling the mixed aerosol population with the aerodynamic lens stack inlet. These soot inclusions within particles mimicking sea salt hydrometeors were formed by externally mixing NaCl aerosols, generated by a nebulized 130 mM solution of NaCl, with spark-generated soot. Using the cascade impactor (see section on MOUDI), these soot particles were size-selected to exclude those larger than 1.8 μm . The mixing of NaCl and soot occurred in a separate chamber prior to the aerodynamic lens stack inlet to minimize the coincidental illumination of distinct soot particles and NaCl particles in the FEL interaction region.

Aerosolized solutions of ellipsoidal nanoparticles (Corpuscular, NY, USA), polystyrene spheres (PostNova Analytics, Germany), NaCl, and other aqueous particles were transported into the lens stack using a pneumatically-assisted sprayer (MiraMist CE, Burgener Research, Inc., Mississauga, Ontario, Canada). These samples were pumped through the sprayer at flow rates ranging from 10–30 $\mu\text{l}/\text{min}$ using an HPLC system (Shimadzu Biotech) while the nitrogen gas flow was kept at 100 psi (~ 1.2 l/min).

Aerosol size-fractionation via MOUDI

A Micro-Orifice Uniform-Deposit Impactor (MOUDI, MSP Corporation, Shoreview, MN) was used as a size selection device in order to control the size of the soot aggregates exiting the Palas GFG100 graphite particle generator. Although the graphite particle generator is specified to create graphite nanoparticles in the range of 20–100 nm, the experimental setup, such as tubing length and gas flow rates cause larger aggregates to form and to make their way into the interaction region. These larger aggregates can clog the aerosol inlet so the MOUDI was implemented as a filtration device to mitigate large particles, but allow smaller particles through to the X-ray interaction region.

The MOUDI is comprised of eight stages with size cutoffs: 9.9 μm , 6.2 μm , 3.1 μm , 1.8 μm , 1.0 μm , 0.55 μm , 0.32 μm , and 0.18 μm . The manufacturer supplied these calibrated values. Each stage is designed to allow passage for particles below its specified filter size. The pressure difference across each stage is key to this size filtration. The holes in each stage do not directly filter the particles, but govern the pressure drop across the stage leading to an increase in the exit velocities of the particles. Whereas smaller particles would follow the streamlines of the airflow, larger particles with too much inertia would not and hence crash onto the plate (Figure S4) excluding them from the next stage. When stages with smaller cutoffs are cascaded, particles of decreasing sizes are obtained. The typical operation of the MOUDI requires a 30 l/min flowrate, supplied by a vacuum pump attached to the MOUDI outlet. During our experimental run, 1 bar of Argon gas was flowing through the spark generator and into the MOUDI. The outlet of the MOUDI was attached to the entrance of the reentrant aerodynamic lens stack, which was at a pressure of 45 Torr.

If all stages were included during a typical run of the MOUDI, the flow exiting the MOUDI would have particles no larger than 0.18 μm . In our soot experiments we would remove some of the lower stages in order to catch many larger aggregates, typically those

larger than 1 μm , to minimize their accumulation at the inlet of the aerodynamic lens stack. The soot aggregates of in Figure 3 were produced without any of the MOUDI stages installed, while those in Figure 4 were subjected to the 1.8 μm filter.

Additional references:

32. Gard, E. *et al.* US Patent 7,361,891 (2006).
33. Schwyn, S. *et al.* Aerosol generation by spark discharge. *J. Aerosol Science* **19:5**, 639-642 (1988).